Nonlinear phase-integral approximations of stationary waves in nonhomogeneous systems

1997 J. Phys. A: Math. Gen. 30 697

(http://iopscience.iop.org/0305-4470/30/2/029)

J. Phys. A: Math. Gen. **30** (1997) 697–710. Printed in the UK PII: S0305-4470(97)75752-4

Nonlinear phase-integral approximations of stationary waves in nonhomogeneous systems

Karl-Erik Thylwe and Harry Dankowicz

Department of Mechanics, Royal Institute of Technology, S-100 44 Stockholm, Sweden

Received 20 June 1996, in final form 24 October 1996

Abstract. A recent normal-form approximation for dynamical equilibria of one-dimensional Hamiltonian systems is shown to provide a phase-integral (WKB) approximation to solutions of nonlinear differential equations. In the present paper, a restricted class of ordinary differential equations $d^2\Psi/dx^2 + h_2(x)\Psi + h_n(x)\Psi^{n-1} = 0, n \geqslant 3$, is considered. The integrability of the truncated normal form allows for expressing the solutions as trigonometric expansions in terms of an 'amplitude' and 'phase'. The method is applied to a Dirichlet boundary value problem on the interval $x \in [x_0, x_1]$ for $n = 3$ and $n = 4$ where the coefficient functions depend on an additional parameter ω. As in the constant coefficient case, we obtain approximate expressions for eigenvalues $\omega_k, k = 1, 2, \ldots$ and eigensolutions near the linear limit. The results show that the interpretative and the predictive power of the linear WKB solutions carry through to the nonlinear regime of small-amplitude, wavelike solutions $\Psi(x)$. We further analyse the mechanism by which the 'odd-n' nonlinearity in general causes a splitting of the linear eigenvalues. In particular, we discuss the singular threshold behaviour of the doubling mechanism for nonlinearities with $n = 3$. If the coefficient functions become constants, the doubling of eigenvalues corresponding to standing waves of odd numbers of nodes gradually disappears. The method of approximation can be worked out similarly for any 'perturbing' polynomial in $\Psi(x)$.

1. Introduction

As a particular application of a recent normal-form theory [1], we consider finding approximate solutions to a class of nonlinear, stationary wave equations

$$d^2\Psi/dx^2 + h_2(x)\Psi + h_n(x)\Psi^{n-1} = 0 \qquad n \geqslant 3. \tag{1}$$

This differential equation appears in various contexts, such as the search for wavelike solutions or stationary solutions to partial differential equations. The linear part of equation (1) has a form suitable for WKB approximations (see a recent review by Fröman and Fröman [2]). The linear WKB theory can handle quite intricate situations with several real and complex transition points (i.e. zeros or singularities of $h_2(x)$) on, or near the interval of x-values relevant in a particular problem. If the linear coefficient is slowly varying and/or its value is large for almost all x, then the approximation is expected to be successful. Such successes are well documented and have been accompanied by detailed semiclassical descriptions of quantal spectroscopy and scattering phenomena. The approximation has also contributed to the understanding of the linear stability problem [3] and the asymptotics of 'special functions' defined by second-order ordinary differential equations [2].

In the nonlinear context of this article, we do not restrict the treatment to the particular situations with periodic coefficients and/or with the linear coefficient having turning points

0305-4470/97/020697+14$19.50

of importance. In both cases, asymptotic matching at (real or complex) transition points is an important element and this is outside the scope of the present article. Here we will assume $h_2(x) > 0$ and that the usual WKB approximation applies to the linearized problem. The remaining coefficient $h_n(x)$ is a quite arbitrary, smooth function of x.

A particular feature of the differential equation (1) is that it can be fitted into a canonical formalism where x replaces time. In fact, it can be derived from the underlying Hamiltonian

$$H(\mathrm{d}\Psi/\mathrm{d}x, \Psi, x) = \tfrac{1}{2}(\mathrm{d}\Psi/\mathrm{d}x)^2 + \tfrac{1}{2}h_2(x)\Psi^2 + \tfrac{1}{n}h_n(x)\Psi^n. \tag{2}$$

With this Hamiltonian at hand there is still no immediate solution to the problem. In the case of periodic coefficients, we can apply a normal-form theory to simplify the Hamiltonian to the extent that the corresponding canonical equations can be trivially solved. These solutions can subsequently be transformed back to give the solution in the original variables. Fortunately, a similar normal-form (canonical perturbation) theory exists also in the case of nonperiodic coefficients. In this short outline of the approximation method we only summarize the essential first-order transformation between the 'final' and 'initial' canonical variables and will refer heavily to the presentation in [1]. In the linear (small-amplitude) limit, the resulting formulae correspond to the celebrated first-order WKB approximation.

The text is organized as follows. Section 2 summarizes the Lewis transformation and the normal form theory of Thylwe and Dankowicz [1] and gives explicit expressions for the approximate solutions derived within this theory. In section 3 we study a class of boundary value problems and show how the nonlinear theory developed in this paper provides an analogy to the traditional, linear WKB method. To illustrate the fundamental ideas and make some of the later results more plausible section 3.1 describes a well known parabolic partial differential equation and its stationary solutions. In the present context this example corresponds to the constant coefficient case, which allows exact, although perhaps not too illucidating, closed form solutions. Finally, section 4 concludes this paper with a summary and suggestions for further study.

2. The normal form

2.1. First-order truncation

The normal form theory of Thylwe and Dankowicz [1] involves no further approximation beside the normal-form truncation. It describes how to simplify the Hamiltonian (2) through a series of canonical transformation. To first order the resulting truncated Hamiltonian can be expressed in terms of the first-order, modified action-angle (Lewis) variables $(\mathcal{L}_1, \phi_1)$:

$$\mathcal{K}_{TD}(\mathcal{L}_1, x) = \eta_1(x)\mathcal{L}_1 + \eta_m(x)\mathcal{L}_1^m \qquad m = n/2 = 2, 3, \ldots \tag{3}$$

for the case of even n, while the second term on the right is absent for nonlinearities of odd powers n. In this representation the phase variable ϕ_1 is cyclic to the order of truncation considered. Consequently, $\mathcal{L}_1$ is an approximate constant of motion, as is typical in action-angle formulations. However, in this case the instantaneous 'angular frequency' (or perhaps more appropriately, the 'local wavenumber') depends explicitly on the position x. Given the truncated Hamiltonian (3), we thus obtain:

$$\frac{\mathrm{d}\phi_1(x)}{\mathrm{d}x} = \eta_1(x) + m\eta_m(x)\mathcal{L}_1^{m-1}. \tag{4}$$

Hence, we directly obtain the solutions

$$\mathcal{L}_1 = \text{constant} \tag{5}$$

and

$$\phi_1(x) = \int^x [\eta_1(x) + m\eta_m(x)\mathcal{L}_1^{m-1}]\mathrm{d}x \tag{6}$$

where ϕ_1 is determined up to a constant angle.

A convenient formulation of the TD normal form utilizes the complex variable

$$Z = \sqrt{2\mathcal{L}_1}\exp(\mathrm{i}[\phi_1(x) + \beta]). \tag{7}$$

The dependence of the solution on initial or boundary conditions comes in through the value of the invariant $\mathcal{L}_1$ and the initial phase β (conveniently made explicit here). Without loss of generality we henceforth assume that $\phi_1(x_0) = 0$ leaving all arbitrariness in β. Since initial or boundary conditions are given in terms of the original variables, we also need the explicit canonical transformations involved; we return to this below.

In the Hamiltonian (3), the η-coefficients depend nontrivially on the original h-coefficients. The leading coefficient $\eta_1(x)$ is shown to be [1]:

$$\eta_1(x) = \rho^{-2}(x) \tag{8}$$

defined by a suitable solution of the Milne equation [4, 5] (see also an early paper by Ermakov [6]), which contains $h_2(x)$ as a coefficient:

$$\frac{\mathrm{d}^2\rho}{\mathrm{d}x^2} + h_2(x)\rho = \frac{1}{\rho^3}. \tag{9}$$

In the present context of generalizing the well known linear WKB, or WKB approximation, the suitable Milne solution is one given by an adiabatic expansion of ρ^{-2}. Formally, one can construct the expansion as described by Fröman and Fröman [2], where they use the explicit differential equation for $q \stackrel{\mathrm{def}}{=} \rho^{-2}$. This choice of expansion appears natural in the phase function and the result then corresponds to the usual WKB approximation in the linear limit. To leading adiabatic order (sufficient for the present outline) the procedure simply amounts to neglecting the derivative in the Milne equation. Hence, in the following development we take the solution

$$\rho_0(x) = \left[1/h_2(x)\right]^{\frac{1}{4}}. \tag{10}$$

This means, in particular, that the first nontrivial normal-form coefficient $\eta_1(t)$ becomes

$$\eta_1(x) \approx \sqrt{h_2(x)}. \tag{11}$$

Since, by assumption, $h_2 > 0$, $\sqrt{h_2(x)}$ has no singularities or branch cuts on the part of the real x-axis of interest. Suitable generalizations will be discussed elsewhere.

We proceed to discuss the coefficient of the nonlinear term in the normal-form Hamiltonian. The normal-form theory does not remove all the nonlinearity in the original Hamiltonian. Some 'diagonal' parts, generated by even-order terms in the original Hamiltonian (2), remain in the transformed Hamiltonian. The coefficient of the leading-order contribution is given by

$$\eta_m = \frac{1}{2m}h_{2m}(x)\rho^{2m}(x)\left(\frac{1}{2}\right)^m\binom{2m}{m} \qquad m = 2, 3, \cdots. \tag{12}$$

The adiabatic approximation (10) of the Milne equation leads to a consistent approximation also for this coefficient. While only the even-order nonlinearities contribute explicitly to the transformed Hamiltonian, we shall see later that the odd-order nonlinearities appear in the canonical transformations.

2.2. New and old variables

The first-order Lie transformation (see [1, 9] for details) relates the solution in the transformed variables to the original ones. To facilitate its application one introduces the auxiliary complex variable

$$z = [\Psi'(x)\rho(x) - \Psi(x)\rho'(x)] + \mathrm{i}\Psi(x)\rho^{-1}(x). \tag{13}$$

The near-identity transformation now becomes

$$z = Z + \{w_1, Z\} \tag{14}$$

where Z is given in terms of the Lewis variables in equation (7). Here, w_1 is a function of Z and Z^* and the Poisson bracket is with respect to the conjugate pair (Z^*, Z).

The ansatz for the Lie generating function w_1 in (14) is chosen to cancel off-diagonal terms in the original Hamiltonian and, hence, is a sum of monomials of degree n, i.e.

$$w_1 = \sum_{l=0}^{n} a_{n-l,l}(x) Z^{n-l} Z^{*l} \qquad l \neq n/2. \tag{15}$$

Symmetries in the relevant expressions (see [1]) imply that $a_{l,n-l} = -a^*_{n-l,l}$. Rigorously, the coefficients in the generating function have to satisfy a differential equation in order to accomplish the desired canonical transformation. As before, however, we again introduce an adiabatic approximation to the equation.

We have for $l \neq n/2$ (see [1]):

$$\frac{\mathrm{d}\, a_{n-l,l}}{\mathrm{d}x} + \mathrm{i}(n-2l)\rho^{-2} a_{n-l,l} = 2\mathrm{i}\frac{h_n \rho^n}{n}\left(-\frac{\mathrm{i}}{2}\right)^n \binom{n}{l}(-1)^l \tag{16}$$

and an adiabatic argument (slowly varying coefficients) yields the leading approximation

$$a_{n-l,l}(x) = \mathrm{i}^n 2^{-(n-1)} \frac{h_n(x)\rho_0^{n+2}(x)}{n} \binom{n}{l} \frac{(-1)^{n+l}}{(n-2l)}. \tag{17}$$

Note that in an exact treatment, there is no unique solution for the coefficients. Typically one would then prefer the smoothest coefficient, and this should be close to the adiabatic one, if it exists.

2.3. Explicit formulae

Next we give some explicit results for the low-order powers $n = 3$ and 4 of the nonlinearity in the differential equation.

$n = 3$: we summarize the key quantities and give the final solution in each case.

$$\eta_m = 0 \tag{18}$$

$$a_{3,0}(x) = a_{0,3}(x) = \frac{\mathrm{i}h_3}{36\, h_2^{5/4}} \stackrel{\text{def}}{=} \mathrm{i}d_{3,0} \tag{19}$$

$$a_{2,1}(x) = a_{1,2}(x) = -\frac{\mathrm{i}h_3}{4\, h_2^{5/4}} \stackrel{\text{def}}{=} -\mathrm{i}d_{2,1} \tag{20}$$

$$z = Z + a_{2,1}Z^2 + 2a_{1,2}ZZ^* + 3a_{0,3}Z^{*2} \tag{21}$$

$$\Psi(x) = \sqrt{2\mathcal{L}_1}h_2^{-1/4}\sin(\phi_1 + \beta) + 2\mathcal{L}_1 h_2^{-1/4}[3d_{3,0}\cos(2\phi_1 + 2\beta) - d_{2,1}(2 + \cos(2\phi_1 + 2\beta))]. \tag{22}$$

Note that the transformation coefficients $a_{n-l,l}$ are imaginary and $d_{n-l,l}$ are real here. From these expressions it is clear that $\sqrt{2\mathcal{L}_1}$ acts as a small parameter, measuring the amplitudes

of the waves while keeping track of the relative order of magnitude between linear and nonlinear contributions. Similar expressions are obtained for all odd nonlinearities.

$n = 4$: in this case the same quantities are

$$\eta_2 = \frac{3\,h_4}{8\,h_2} \tag{23}$$

$$a_{4,0}(x) = -a_{0,4}(x) = \frac{h_4}{128\,h_2^{3/2}} \tag{24}$$

$$a_{3,1}(x) = -a_{1,3}(x) = -\frac{h_4}{16h_2^{3/2}} \tag{25}$$

$$z = Z + a_{3,1}Z^3 + 3a_{1,3}ZZ^{*2} + 4a_{0,4}Z^{*3} \tag{26}$$

$$\Psi(x) = \sqrt{2\mathcal{L}_1}h_2^{-1/4}(x)(\sin(\phi_1+\beta)+2\mathcal{L}_1[(a_{3,1}+4a_{4,0})\sin(3\phi_1+3\beta)+3a_{3,1}\sin(\phi_1+\beta)]). \tag{27}$$

Recall that the coefficients are real here and that the index symmetry changes. The realness of the coefficient has the consequence that the cosines convert to sines here. We also note that all nonlinear contributions are 'oscillatory', contrary to a non-oscillatory contribution present in the previous case. Again, this is true for all even nonlinearities.

3. A nonlinear phase-integral (NPI) approximation

In this section we apply the above theory to a class of boundary value problems. We will describe the similarities between the nonlinear theory developed in this paper and the traditional WKB approximation mentioned in section 1. The stage for the nonhomogeneous analysis is set by first restricting attention to the case of constant coefficients depending on an unknown parameter ω. In particular, the existence of solutions depended on the value of the parameter. We will refer to values of ω for which solutions exist as eigenvalues and the corresponding solutions as eigensolutions.

Following the constant coefficient discussion, in the nonhomogeneous situation we begin by illustrating the linear case and proceed to analyse the effect of even-n nonlinearities, represented by $n = 4$. The odd-n nonlinearities, represented by $n = 3$, cause a somewhat more detailed analysis of the spectrum, which is related to a doubling mechanism.

In the following discussion we use Dirichlet boundary conditions:

$$\Psi(x_0, \omega) = \Psi(x_1, \omega) = 0. \tag{28}$$

In general, these conditions will in turn restrict the possible values of the parameter ω.

3.1. The constant coefficient case

We consider the real Ginzburg–Landau equation in one spatial dimension on the finite domain $[0, L]$.

$$u_t = u_{xx} + h_2(\omega)u - h_4(\omega)u^3. \tag{29}$$

Here, the coefficient functions are functions of an unknown parameter ω only, and $h_2, h_4 > 0$. Versions of this equation appear as a normal form in bifurcation studies for generic parabolic partial differential equations as well as in actual physical applications (see for example [7] and [8]). We will assume Dirichlet boundary conditions at the domain

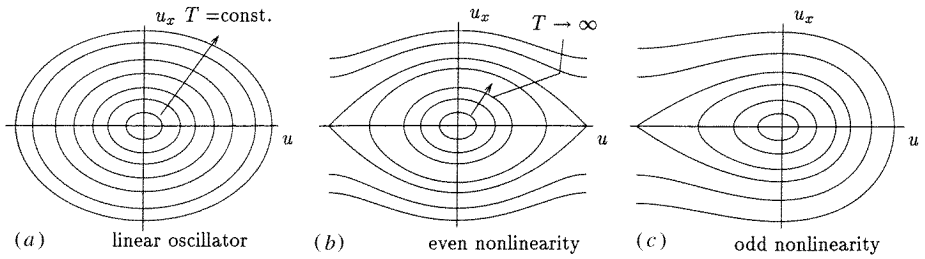

Figure 1. Phase portraits for linear and nonlinear oscillators. Note the dependence of the period on the amplitude and its implications on the existence of solutions of the boundary value problem.

boundaries. In particular, stationary solutions correspond to orbits in (u, u_x) space of the undamped Duffing equation

$$u_{xx} + h_2(\omega)u - h_4(\omega)u^3 = 0 \tag{30}$$

with initial and final states on the $u = 0$ axis.

As a first approximation we neglect the nonlinear term and draw a phase portrait for the corresponding harmonic oscillator (see figure 1(*a*)). Since the period of the oscillations around the origin is independent of the amplitude and only depends on ω, it follows that for a given value of ω, we either have no solutions or a continuum of solutions for all values of the amplitude. In fact, solutions exist only for discrete values of $h_2(\omega)$.

In the nonlinear case, (see figure 1(*b*)), the period for bounded motion depends on the amplitude of the motion. In particular, the period goes to infinity as the initial conditions approach the separatrix. Thus, for a given value of ω there is a largest amplitude and a related infinite family of discrete amplitudes corresponding to solutions to the boundary value problem. As the amplitude decreases the number of turns around the origin increases correspondingly. Continuous variations of ω lead to continuous variations of the allowed values of the amplitudes. In this case solutions exist for intervals of $h_2(\omega)$.

If we further impose a condition on the slope of the solution at the left boundary, solutions only exist for discrete values of $h_2(\omega)$. This is also a natural restriction when numerically searching for solutions. In the present case, we note that the symmetry about the vertical axis implies that given a solution with a prescribed slope $u'(0)$ and parameter value ω, there is a solution with slope $-u'(0)$ and the same value for ω. This is not the case when the symmetry is broken. For example, the odd-n nonlinearity, here exemplified by the ordinary differential equation

$$u_{xx} + h_2(\omega)u + h_3(\omega)u^2 = 0 \tag{31}$$

(see figure 1(*c*)) results in a splitting between the values of ω corresponding to $u'(0)$ and $-u'(0)$ which grows with the degree of asymmetry. Clearly, the inner orbits, which also have larger winding numbers, correspond to smaller splittings. This sort of symmetry breaking and the corresponding splitting is reminiscent of eigenvalue splitting in quantum mechanics.

The same phenomena will appear in the subsequent discussion, which will provide approximate solutions to problems where the coefficient functions actually depend on x as well as ω. In the study of various types of instabilities and phase transitions in dissipative partial differential equations, the types of stationary solutions we have described are of fundamental use. In particular, their stability under small perturbations is of interest and much research has been devoted to the constant coefficient case.

3.2. Linear phase-integral eigenvalues

If our original equation (1) would be just linear ($h_n(x,\omega) = 0$), the adiabatic approximation of the Milne solution and the identity transformation leads to the usual WKB solution of the original problem

$$\Psi(x,\omega) = \rho_0(x,\omega)\Im Z(x,\omega) = \sqrt{2\mathcal{L}_1}\rho_0(x,\omega)\sin(\phi_1(x,\omega)+\beta) \tag{32}$$

where $\rho_0(x,\omega)$ is given by (10). Note also that the invariant, $\mathcal{L}_1$, is related to the amplitude of the WKB solution. The boundary conditions imply that nontrivial solutions exist only for $\beta = 0, \pi$ and

$$\phi_1(x_1,\omega) = k\pi \qquad k = 1, 2, \ldots. \tag{33}$$

The eigenvalues, ω_k, are obtained as solutions to this equation. Since $\phi_1(x_1,\omega)$ is independent of the amplitude of the wave, this eigenvalue condition results in no restriction on the possible values of $\mathcal{L}_1$. In linear theories it is standard to arbitrarily normalize the solution, which in turn determines $\mathcal{L}_1$. In addition to labelling the eigenvalues, the index k also has the physical relevance that $(k-1)$ represents the number of nodes of the eigensolution. We note the obvious similarities with the constant coefficient case of the previous section, where k describes the number of times a solution winds around the origin.

3.3. Even-n NPI eigenvalues

We now look at the eigenvalue problem corresponding to the nonlinearity $n = 4$. From the explicit solution (27), the left boundary condition of the wave implies

$$0 = \sin(\beta)[1 + 2\,\mathcal{L}_1[(a_{3,1}(x_0,\omega) + 4a_{4,0}(x_0,\omega))(3 - 4\sin^2(\beta)) + 3\,a_{3,1}(x_0,\omega)]]. \tag{34}$$

This condition is satisfied by $\beta = 0$ (and π) independently of the value of $\mathcal{L}_1$. We notice that, if $\mathcal{L}_1$ is sufficiently large, other solution of β may come into play. However, since the approximation is only valid for small-amplitude waves, these values will not be considered.

We now impose the boundary condition at $x = x_1$ to obtain

$$\begin{aligned} 0 = {} & \sin(\phi_1(x_1,\omega)) \\ & \times[1 + 2\,\mathcal{L}_1[(a_{3,1}(x_1,\omega)+4a_{4,0}(x_1,\omega))(3 - 4\sin^2(\phi_1(x_1,\omega))+3a_{3,1}(x_1,\omega)]]. \end{aligned} \tag{35}$$

Again, we obtain the compact eigenvalue condition

$$\phi_1(x_1,\omega_k) = k\pi \qquad k = 1, 2, \ldots. \tag{36}$$

We recognize from (6) that ϕ_1 depends on $\mathcal{L}_1$ through

$$\phi_1(x_1,\omega) = \int_{x_0}^{x_1}\left[\sqrt{h_2(x',\omega)} + 2\mathcal{L}_1\frac{3\,h_4(x',\omega)}{8\,h_2(x',\omega)}\right]\mathrm{d}x'. \tag{37}$$

For a given value of the 'winding number' k we then obtain a relation between the eigenvalue ω_k and the Lewis invariant $\mathcal{L}_1$.

When searching for waves satisfying the boundary condition (36) we limit ourselves to those within a given (small) amplitude class, specified by $\mathcal{L}_1$. This classification, however, is not exact, and can cause some trouble when comparisons with exact waves have to be made. In particular, the physical significance of the Lewis invariant is not immediate, nor is its value easily related to measurable quantities. In section 3.1 we related the eigenvalues to values of the slope at the left boundary, instead of the 'amplitude'. Since the slope is a measurable quantity of a solution, this enables us to make sensible comparisons between

approximate and exact waves. Using equations (13), (24)–(26) one obtains the following approximate expression for the derivative

$$\Psi'(x_0,\omega) = \sqrt{2\mathcal{L}_1}h_2^{1/4}(x_0,\omega) + \frac{3(2\mathcal{L}_1)^{3/2}}{32\,h_2^{5/4}(x_0,\omega)}h_4(x_0,\omega). \tag{38}$$

For fixed k, this equation together with equation (37) yield a relation between the derivative of the wave at the boundary $x = x_0$ as a function of the eigenvalue ω_k.

To facilitate a comparison between approximate and exact, numerical solutions, we proceed as follows. We fix values of the Lewis invariant, $\mathcal{L}_1$, and the 'winding number', k. The integral condition (37) then yields a value for the NPI eigenvalue, ω_k^{NPI}. Substitutions of this value into equation (38) then results in a value for the slope of the approximate solution at the left boundary. We then impose this value on the slope of exact solutions and vary the parameter ω until an exact, numerical solution is found at which $\omega_k = \omega_k^{\mathrm{exact}}$. This can then be quantitatively compared with the approximate eigenvalue and eigensolution obtained previously.

We illustrate the idea for a model system with

$$h_2(x,\omega) = \omega^2\,(1+x)^2 \tag{39}$$

and

$$h_4(x,\omega) = \omega\,(1+x)^2. \tag{40}$$

Assuming the Dirichlet boundary conditions are on the interval $[0,1]$, and a fixed value of k, we try to find the relation between the eigenvalues $\omega = \omega_k$ and $\mathcal{L}_1$ satisfying these conditions. The integral defining $\phi_1(1)$ in the approximate condition (36) can be solved analytically to yield

$$\frac{3}{2}\omega + \frac{3}{4\,\omega}\mathcal{L}_1 = k\pi. \tag{41}$$

Using equation (41) in equation (38) we find

$$\Psi'(0) = \frac{5}{4}\left(\frac{2k\pi}{3} - \omega\right)^{\frac{1}{2}}\left(\frac{2k\pi}{5} + \omega\right). \tag{42}$$

It is clear that equation (1) together with the given boundary conditions only has solutions for ranges of values of ω. In turn, this implies ranges of the 'amplitude' $\mathcal{L}_1$ for which exact solutions can be found. Since our normal form is only approximately valid for small values of $\mathcal{L}_1$, equation (41) limits our considerations to values of ω near $\frac{2k\pi}{3}$ or 0. The latter can be eliminated by the restriction that the quartic terms be much smaller than the linear terms. In table 1 we list choices of the index k and the Lewis invariant $\mathcal{L}_1$ together with the approximate eigenvalues ω_k^{NPI}. Also shown are the approximate derivatives at the left boundary from equation (42), and the 'exact' eigenvalues, ω^{exact}.

Figure 2 illustrates the amplitude-dependence of the leading eigenvalues ω_k^{NPI} in the $(\omega, \mathcal{L}_1)$-plane. The eigenvalues of the linear theory appear as vertical, broken lines. It is seen for this model that the nonlinear shifts gradually decrease as the nodal number k increases.

In figure 3 we illustrate the approximate and exact solutions found using the described procedure. This graphical comparison together with the fair agreement between approximate and 'exact' eigenvalues in table 1, at least for sufficiently small values of $\mathcal{L}_1$ and larger values of k, lends credibility to the applicability of the normal form developed in this paper. While it is likely that higher-order approximations to the solution of the Milne equation and the ordinary differential equations for the coefficients a_{ij} would lead to a progressively

Table 1. Comparison of NPI eigenvalues with exact ones for the case $n = 4$. Note that the corresponding approximate and exact waves have the same slopes at the left boundary $x = 0$.

$\mathcal{L}_1$	k	$\Psi'(0)$	ω_k^{NPI}	ω_k^{exact}
0.0001	1	0.0205	2.0944	2.0603
0.0001	10	0.0647	20.9440	20.9395
0.0001	100	0.2047	209.4395	209.4391
0.1	1	0.6463	2.0702	2.0382
0.1	10	2.0466	20.9416	20.9371
0.1	100	6.4721	209.4393	209.4388
1	1	2.0157	1.8196	1.8480
1	10	6.4712	20.9201	20.9157
1	100	20.4665	209.4371	209.4367

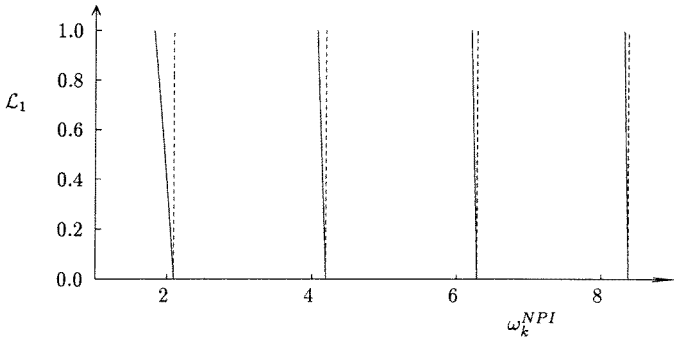

Figure 2. Illustration of the NPI eigenvalue curves $\omega_k(\mathcal{L}_1)$ (full-drawn curves) for the case $n = 4$. The broken, vertical curves refer to the linear theory.

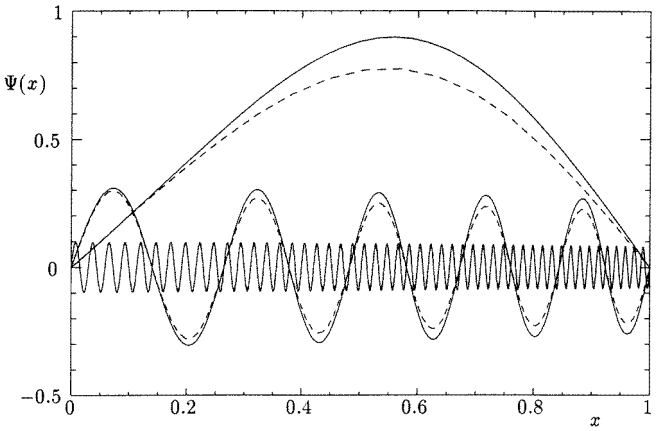

Figure 3. Comparison of approximate (full-drawn) and exact (broken) waves corresponding to $\mathcal{L}_1 = 1$ and $k = 1, 10, 100$.

better agreement (up to some optimal order), we believe that the present theory should suffice in many applications. In particular, the closed form expressions we have obtained lend themselves to a qualitative analysis.

Finally, we suggest using the L^2 norm evaluated over the interval [0, 1] as an alternative comparison between the approximate solution and one found numerically. In the case of the approximate solution this becomes an algebraic expression in the amplitude $\mathcal{L}_1$ which then offers a determination of the appropriate 'amplitude' to be used in the normal form expressions. Moreover, it gives a check for which exact solutions could possibly be approximated by the nonlinear WKB expressions found in this discussion.

3.4. Odd-n NPI eigenvalues

In the present section we perform similar eigenvalue calculations as above for nonlinearities of odd n. The application of the NPI approximation becomes somewhat more complicated in the odd case, the main phenomenon being a splitting of the eigenvalues due to the nonlinearity.

For ease of reference we repeat the relevant expressions from section 2.3. The general solution (22) can be written

$$\Psi(x,\omega) = \sqrt{2\mathcal{L}_1}h_2^{-1/4}(x,\omega) \times \left\{ \sin(\phi_1(x,\omega)+\beta) - \sqrt{2\mathcal{L}_1}\frac{h_3(x,\omega)}{2h_2^{5/4}(x,\omega)}\left[\frac{1}{3}\cos(2\phi_1(x,\omega)+2\beta)+1\right]\right\} \tag{43}$$

where

$$\phi_1(x,\omega) = \int_{x_0}^{x} \sqrt{h_2(x',\omega)}\,\mathrm{d}x'. \tag{44}$$

After simplification, the Dirichlet boundary condition at the left boundary becomes

$$\sin^2\beta + \mathcal{C}(x_0,\omega,\mathcal{L}_1)\sin\beta - 2 = 0 \tag{45}$$

where

$$\mathcal{C}(x,\omega,\mathcal{L}_1) = \frac{3h_2^{\frac{5}{4}}(x,\omega)}{\sqrt{2\mathcal{L}_1}h_3(x,\omega)}. \tag{46}$$

It is easy to show that equation (45) has real solutions only for $|\mathcal{C}(x_0,\omega,\mathcal{L}_1)| > 1$ and is given by

$$\sin\beta = \tfrac{1}{2}(\sqrt{8+\mathcal{C}^2(x_0,\omega,\mathcal{L}_1)} - \mathcal{C}(x_0,\omega,\mathcal{L}_1)) \tag{47}$$

from which we distinguish two initial phases β_0 and $\beta_1 = \pi - \beta_0$, where $\beta_0 \to 0$, as $\mathcal{L}_1 \to 0$.

We now impose the boundary condition at $x = x_1$. This gives the analogous condition:

$$\sin\alpha = \tfrac{1}{2}\left(\sqrt{8+\mathcal{C}^2(x_1,\omega,\mathcal{L}_1)} - \mathcal{C}(x_1,\omega,\mathcal{L}_1)\right) \tag{48}$$

where $\alpha = \phi_1(x_1) + \beta$, and we again require $|\mathcal{C}(x_1,\omega,\mathcal{L}_1)| > 1$. As before, we find two angles (mod 2π) α_0 and $\alpha_1 = \pi - \alpha_0$. Combining the two boundary conditions we obtain four conditions for the phase function $\phi_1(x_1)$:

$$\phi_1(x_1) = \alpha_0 - \beta_0 + 2k_1\pi \tag{49}$$

$$\phi_1(x_1) = \pi + \alpha_0 + \beta_0 + 2k_2\pi \tag{50}$$

$$\phi_1(x_1) = \pi - \alpha_0 - \beta_0 + 2k_3\pi \tag{51}$$

$$\phi_1(x_1) = -\alpha_0 + \beta_0 + 2k_4\pi \tag{52}$$

where k_1, k_2, k_3, k_4 are any integers consistent with $\phi_1(x_1) > 0$. We formally rewrite the conditions in the compact form

$$\phi_1(x_1) = \pm[\alpha_0 + (-1)^{k+1}\beta_0] + k\pi \qquad k = 1, 2, 3, \ldots. \tag{53}$$

In this way we get twice as many eigenvalues as in the linear and 'nonlinear even' cases, like a splitting of degenerate levels. In the case discussed in section 3.1, $\alpha_0 = \beta_0$ by symmetry of the boundary conditions. Two of the four eigenvalue conditions then degenerate (collapse) into one, but the remaining two conditions survive as long as the system is nonlinear. We can combine the two conditions to yield a relation between the Lewis invariant, $\mathcal{L}_1$, and the parameter ω as in equation (41). The defining relation $\phi_1(x_1, \omega) = \alpha - \beta$ implies that

$$\sin\phi_1(x_1, \omega) = \sin\alpha\cos\beta - \sin\beta\cos\alpha. \tag{54}$$

The left-hand side of this equation can be written as a function of ω. Similarly, we may use equations (47) and (48) to express the right-hand side in terms of ω and $\mathcal{L}_1$. We note that the sign of $\cos\beta$ depends on whether $\beta = \beta_0$ or $\beta = \beta_1$ and similarly for $\cos\alpha$.

Furthermore, we may proceed to express the slope at the left-hand boundary in terms of ω and $\mathcal{L}_1$. Formally eliminating $\mathcal{L}_1$ from these relations yields a relationship between ω and $\Psi'(0)$ as in equation (42). Using this, a straightforward comparison between exact and approximate solutions is made possible in the same fashion as in the previous section.

We apply the above discussion to the model system

$$h_2(x) = \omega^2\,(1 + x)^2 \tag{55}$$

and

$$h_3(x) = \omega\,(1 + x)^2 \tag{56}$$

in order to compare numerically obtained, 'exact' eigenvalues ω_k^{exact} and approximate eigenvalues ω_k^{NPI}.

Table 2. Comparison of NPI eigenvalues and exact ones for the case $n = 3$. Note that the corresponding approximate and exact waves have the same slopes at the left boundary $x = 0$.

$\mathcal{L}_1$	k	$\Psi'(0)$	ω^{NPI}	ω^{exact}
0.0001	1	−0.0207	2.0979	2.0637
0.0001	1	0.0207	2.0908	2.0570
0.0001	10	−0.0637	20.9440	20.9395
0.0001	10	0.0637	20.9439	20.9395
0.0001	100	−0.2047	209.4395	209.4391
0.0001	100	0.2047	209.4395	209.4391
0.1	1	−0.6711	2.1983	2.1700
0.1	1	0.6369	1.9723	1.9601
0.1	10	−2.0473	20.9446	20.9402
0.1	10	2.0473	20.9433	20.9390
0.1	100	−6.4289	209.4395	209.4391
0.1	100	6.4289	209.4395	209.4390
1	1	−2.2667	2.3815	2.4437
1	1	1.9478	1.5824	1.7681
1	10	−6.4747	20.9459	20.9427
1	10	6.4741	20.9420	20.9389
1	100	−20.3301	209.4396	209.4391
1	100	20.3301	209.4394	209.4390

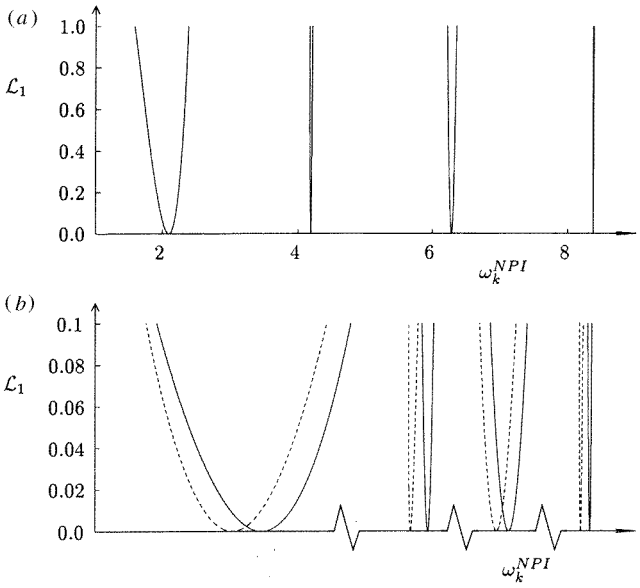

Figure 4. Illustration of the NPI eigenvalue curves $\omega_k(\mathcal{L}_1)$ (a) for the case $n = 3$ and (b) enlargement of (a) providing a detailed comparison with exact eigenvalue curves (broken) near the linear limit.

Table 2 shows the numerical values of the sample calculations. The higher eigenvalues of each doublet are associated with the negative derivative of the wave at the left boundary. This is due to the nonlinearity slowing down the oscillation on the negative branch. The asymmetry effect is partially cancelled if the wave has deflections into the positive branch. The lowest modes have no nodes, which then causes a particularly large eigenvalue difference between the purely negative deflection mode and the purely positive one. Consequently, all odd numbers k (corresponding to waves with $(k-1)$ nodes) are associated with comparatively larger splittings, which also remain when the coefficient functions in the differential equation become constants.

Figure 4 illustrates the amplitude dependence of the eigenvalue splitting for ω^{NPI}, $k = 1, 2, 3, 4$, with a detailed comparison with exact calculations (broken lines). Generally the nonlinear effects decrease as k becomes larger for this model, since the actual amplitudes ($\mathcal{L}_1$= constant) of the waves decrease with k. However, the odd-k waves are seen to have comparatively larger splittings. On a detailed level the nonlinear WKB approximation seems to reproduce the widths of the eigenvalue splittings quite accurately. The lower subplot indicates merely an overall shift of the approximate and exact eigenvalue curves.

The quite dramatic threshold dependence of the splitting effect (best seen for $k = 1$) is expected only for the Hamiltonian nonlinearity of the power $n = 3$. In fact, we can see already from the explicit formulae for the waves, given in section 2.3, that the nonlinear contributions to the waves are proportional to $\mathcal{L}_1^{(n-2)/2}$. Since the resulting shifts in the eigenvalues are expected to be proportional to the same 'small parameter', as $\mathcal{L}_1 \to 0$, the singular nonlinear threshold behaviour occurs only for $n = 3$.

Figure 5 also examines the details of the waves corresponding to a 'doublet' with $k = 3$ and $\mathcal{L}_1 = 1$. The absolute values of the NPI waves are used in the upper subplot and the corresponding exact waves are in the lower subplot. A comparison with the exact curves

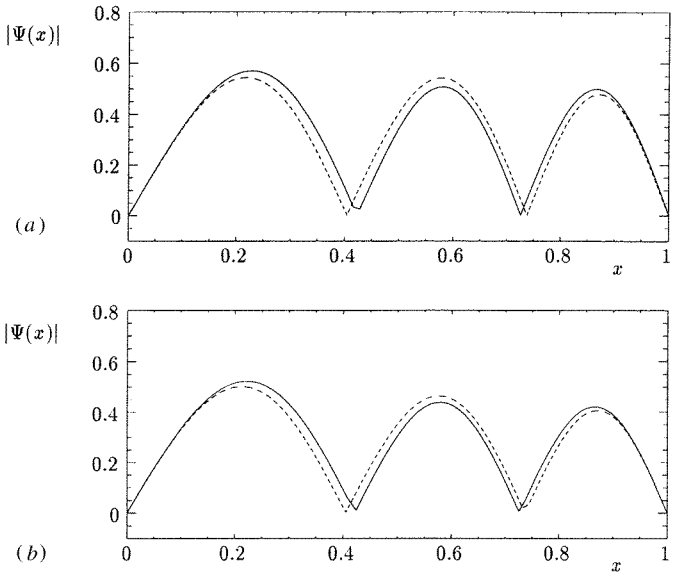

Figure 5. Graphical analysis of the absolute values of the doublet waves corresponding to $\mathcal{L}_1 = 1$ and $k = 3$. Approximate (exact) waves are in the upper (lower) subplot. The doublet wave with the larger of the eigenvalues in our model is illustrated by full-drawn curves. The approximate waves are seen to correctly predict deviations of nodal positions and local deflections.

shows that the relative structures of the doublet waves are well reproduced by the NPI approximation.

4. Conclusions

In this paper the normal-form theory of Thylwe and Dankowicz [1] has been shown to provide a basis for generalizing the linear WKB approximation to a nonlinear context. We observed that good approximations to exact solutions could be obtained and that even better eigenvalue calculations could be performed in this nonhomogeneous situation.

We have further studied a doubling of parameter eigenvalues by analysing the NPI condition for the case of odd-n nonlinearities. The characteristics of the nonlinear doubling is different for waves of odd and even numbers of nodes. The width of the splitting is accurately predicted by the approximate formulae, even if this is sometimes smaller than the absolute displacement of the eigenvalue caused by the approximations. The kind of (systematic) errors involved in this WKB approximation do not seem to destroy the description of small shifts. Similar observations have been made in the linear WKB theory [10].

In the present paper the degree of approximation has been twofold. In addition to obtaining a truncated normal form Hamiltonian we have further restricted ourselves to an adiabatic treatment. In particular the adiabatic solution of the Milne (amplitude) equation has been chosen as a basis for the development. The uniform validity of this approximation is related to analytic properties of the coefficient function $h_2(x)$. The general experience is that real and almost real zeros of $h_2(x)$ deteriorate the adiabaticity. This is particularly subtle when $h_2(x)$ is a periodic function, in which case zeros with large imaginary parts may still cause nonadiabatic resonances [3]. With these restrictions in mind, the adiabatic approximation is expected to be good.

Although we have not treated higher-order approximations, these fit very well into the same formalism. On one hand, Milnes equation generates the expansion:

$$\rho^{-2}(x) = \rho_0^{-2}(x)(1 + Y_2(x) + Y_4(x) + \cdots) \tag{57}$$

in analogy with the expansion functions of Fröman and Fröman [2]. This expansion, in turn, generates an expansion of the transformation coefficients and the extra phase function $\eta_m(x)$. On the other hand, the higher-order Lie transform [1] just adds new terms in the wave, containing higher multiples of the phase functions. The corresponding new coefficient functions can be expressed in terms of the previously determined ones. While it is possible to carry the method further in order to attempt at a higher accuracy in approximating exact solutions, this has not been undertaken in the present text. It is our belief that the method has been adequately illuminated without this additional degree of accuracy and further expect the present lower-order approximation to be sufficient in many situations of practical importance.

The problem with transition points has not been considered here. However, this is an important task for the wider applicability of the NPI approximation. Already the inclusion of a single (real, or almost real) transition point, for example, may lead to new insights of nonlinear wave reflection phenomena. As previously mentioned, such transition points between essentially stable ($h_2 > 0$) and unstable ($h_2 < 0$) regions would require some sort of matching between approximate solutions in neighbouring regions.

The method developed in this paper is of significance in various physical contexts. In certain simplified models of electromagnetic wavepropagation the nonlinear Schrödinger equation plays a central role. In these situations, the matching at transition points is a desired element. In other situations such as pattern formation and instabilities in infinite dimensional systems, equations of the fundamental form (1) appear in searching for stationary solutions of nonhomogeneous, dissipative partial differential equations. To apply stability theory to these approximate solutions to aid in a more extensive bifurcation investigation would be of particular interest.

Acknowledgments

Financial support by the Swedish Natural Research Council (K-E Thylwe) and the Göran Gustafsson Foundation (H Dankowicz) is gratefully acknowledged.

References

[1] Thylwe K-E and Dankowicz H 1996 *J. Phys. A: Math. Gen.* **29** 3707
[2] Fröman N and Fröman P O 1996 *Phase-Integral Method: Allowing Nearlying Transition Points (Springer tracts in natural philosophy)* vol 40 (New York: Springer) ch 2
[3] Thylwe K-E and Gravador E 1995 *J. Sound. Vibr.* **182** 191
[4] Milne W E 1930 *Phys. Rev.* **35** 863
[5] Thylwe K-E and Bensch F 1994 *J. Phys. A: Math. Gen.* **27** 7475
[6] Ermakov V 1880 *Univ. Izv. Kiev, Serie III* **9** 1
[7] Collet P and Eckmann J-P 1990 *Instabilities and Fronts in Extended Systems* (Princeton, NJ: Princeton University Press)
[8] Temam R 1988 *Infinite-Dimensional Dynamical Systems in Mechanics and Physics* (New York: Springer)
[9] Cary J R 1981 *Phys. Rep.* **79** 129
[10] Amaha A and Thylwe K-E 1994 *Phys. Rev.* A **50** 1420